The Sensitivity of V_2O_5:Sm_2O_3 Thin Films against NO_2 Toxic Gas

A.J. Noori[1*], R.A. Ahmed[2], I.M. Ibrahim[3]

Abstract

Vanadium oxide V_2O_5 thin films with variation doping ratios of Sm_2O_5 (2, 4, 6, and 8 % wt.) on corn glass and p- type silicon substrates were prepared by pulsed laser method. The X-ray diffraction peaks for V_2O_5 decreases with doping ratio of Sm_2O_3. FESEM images for V_2O_5 and doped thin films illustrates clusters with a homogeneous distribution in nano scale. The energy gap varied upon the increment of doping concentration, starting from 2.610 eV to 2.7 eV. Gas sensor measurement of pure and doped V_2O_5 demonstrated a sensitivity to NO_2 gas, and the sensitivity expanded upon the increment of operation temperature. The greatest sensitivity was found to be about 99%, while best response time of 10s and recovery time of 18s were recorded using the 4% Sm_2O_3 sample at 50 °C.

Key Words: Thin Film, Nano, Structures, Gas Sensor.

DOI Number: 10.14704/nq.2021.19.3.NQ21030 **NeuroQuantology 2021; 19(3):69-77**

Introduction

Many oxidation states of vanadium give rise to a wide variety of oxides. The oxides of the claimed vanadium have a complex stoichiometric composition. Concerning this research, vanadium pentoxide V_2O_5 has a large application among those metal oxide semiconductors, vanadium pentoxide draws huge enthusiasm through as far back as decades owing should its broad assortment of utilizations. Its multivalency, layered structure, optical band gap, chemical and thermal stability, very good thermoelectric characteristic, and so on are the properties that make activate vanadium pentoxide V_2O_5 an ensuring material for demands in microelectronics, electrochemical and optoelectronic appliance. It could a chance to be utilized concerning illustration a gas sensor, a window for solar cell and electrochromic gadgets and in addition optical switches, yet all there need been a developing enthusiasm toward the creation of thin film batteries (TFB) (Benmoussa et al., 2002). V_2O_5 is the greater part stable oxide furthermore indicates semiconductor characteristic for an energy gap of ~ 2.2 e V (Zou and Gao 2010). There are two bulk structures for vanadium pentoxide, the first one is α-V_2O_5 and the second one is ɣ-V_2O_5. The structure of α-V_2O_5 is orthorhombic layered structure. Pyramid structural plane expands for five oxygen molecules encompassing one V molecule (Londero and Schröder 2010; Ali et al., 2018).

Samarium oxide (Sm_2O_3) nanoparticles, prominently known as SM-MITE powders, are accessible in covered and hydrophilic forms. Samarium belongs to block F, Period 6 while oxygen belongs to block P, Period 2 of the periodic table.

Gas sensor examination of V_2O_5:Sm_2O_3 thin film with concentration (2,4,6,8) wt.% were prepared using pulsed laser deposition on glass. This examination depends on the adsorption of gas molecules on the surface of the material which increase with increasing of surface to volume ratio (Bhushan 2007).

Corresponding author: A.J. Noori
Address: [1*]Directorate of Kirkuk Province Education, Kirkuk, Iraq; [2]General Directorate of Education Salah Din, Education Department of Tuz, Iraq; [3]Department of Physics, College of Science, University of Baghdad, Baghdad, Iraq.
[2]E-mail: daloahmed@gmail.com
Relevant conflicts of interest/financial disclosures: The authors declare that the research was conducted in the absence of any commercial or financial relationships that could be construed as a potential conflict of interest.
Received: 05 February 2021 **Accepted:** 05 March 2021

The sensitivity is determined by the change in resistance when the sensor is exposed to a certain gas concentration. The sensitivity can be determined from (Bochenkov and Sergeev 2010):

$$S = \left|\frac{R_g - R_a}{NR_a}\right| \times 100\% \qquad (1)$$

where (R_a) and (R_g) are electric resistance of sensor over air and in presence of gas respectively, (N) will be the gas concentration. The response time of the sensor is characterized by change that takes those sensors should to achieve 90% of max/min worth of resistance upon introduction of the reducing /oxidizing gas (Gibbs et al., 2013).

Experimental

V_2O_5 nanoparticles with different doping concentrations of Sm_2O_3 (2, 4, 6 and 8) wt.% with high purity of 99.999 % is pressed under pressure of 5 tons to form a target of 1.5 cm diameter and 0.2 cm thickness. It should be as dense and homogeneous as much as possible to ensure a good quality of the deposit. In the Pulsed Laser Deposition (PLD) technique, which is a setup of 200 mJ with constant shoot of 600 are carried out. The distance between the target and the substrate is 2 cm, while the distance between the target and the laser source is 12 cm, the laser may be kept tabs onto a pivoting target the place it evaporates those material to structure a plume. The plume goes Previously, possibly vacuum or gas foundation area the middle of those target and the substrate When depositing on the substrate to structure a film. Those methodology is preceded toward those clearing of the chamber to a high vacuum, those PLD method need been demonstrated on a chance to be a successful system should store high-quality films, Uniform thin films, The intricate material films what's more secondary controllability of arrangement of dainty thin films, (Isam et al., 2018). V_2O_5:Sm_2O_3 thin film have been readied by PLD system. The pulsed laser deposition with a vacuum chamber generally at (10^{-3} Torr) vacuum conditions, the target is putted Infront to the Nd: YAG Q - switching laser beam with angle 45°. The thickness about of 100 nm where measurements by weighting method. The samples then annealed up to 400°C for one hour in the vacuum oven.

The structural and morphological experiments are containing X-ray diffraction, field emission scanning electron microscope X-ray diffractions using a Philips X-ray diffractometer system. The X-ray diffraction (XRD) pattern of the (V_2O_5) and (V_2O_5:Sm_2O_3) film deposited on Si substrate toward SHIMADZU XRD -6000 X-ray diffract meter [CuK_α radiation λ=0.154 nm] done 2θ range from on. The interplaner distanced d_{hkl} for different planes are measured.

Field Emission Scanning Electron Microscopy (FESEM) Vega TOSHIBA S 4160 where used for measuring the prepared samples. The absorption spectrum for V_2O_5 with different doping centralization of Sm_2O_3 films once glass substrate is measured utilizing OPTIMA SP_3000 UV_VIS spectrophotometer covering a range from 190 to 1100 nm utilizing glass substrates as a reference gas sensor detector namely, reaction time also recuperation run through. To this end as setup demonstrated.

Those varieties of the sensor resistance when presented to air_NO_2 gas ratio volumetric concentration of 10% gas to air ratio.

The test gas through a flow meter, furthermore needle valve plan. The blending gas is fed may be fed through a tube again those sensors inside those test chamber to give acceptable those true sensitivities.

Results and Discussion

Figure 1 indicates the X-ray diffraction patterns of deposit V_2O_5 thin films on Si substrates with orientation (111) by PLD technique with different doping concentrations of Sm_2O_3 (2, 4, 6 and 8) wt.%, we have to mention here that we used the Si substrate to get more crystallinity than amorphous substrate. Hall measurements show that all these films have a negative Hall coefficient (n type charge carriers), this is attributed may be due to the number of electrons excited above the conduction band mobility edge is larger than the number of holes excited below the valance band mobility edge. The peak of Si located at 2θ= 28.1 ° which related (111) direction. At (2 and 4) wt. % Sm_2O_3 tests their two peaks spotted at (2θ= 32° with 41°) which correspond to ($1\bar{1}1$),(301) direction, respectively for Diffraction information ICDD (96-101-0341), for V_2O_5 crystals, same time there would different peaks show up In (6, and 8) wt. % Sm_2O_3 at (2θ=45.0259°, and 51.2468°) alluded will {($1\bar{0}3$) and (020)} direction, respectively, to Sm_2O_3 crystals.

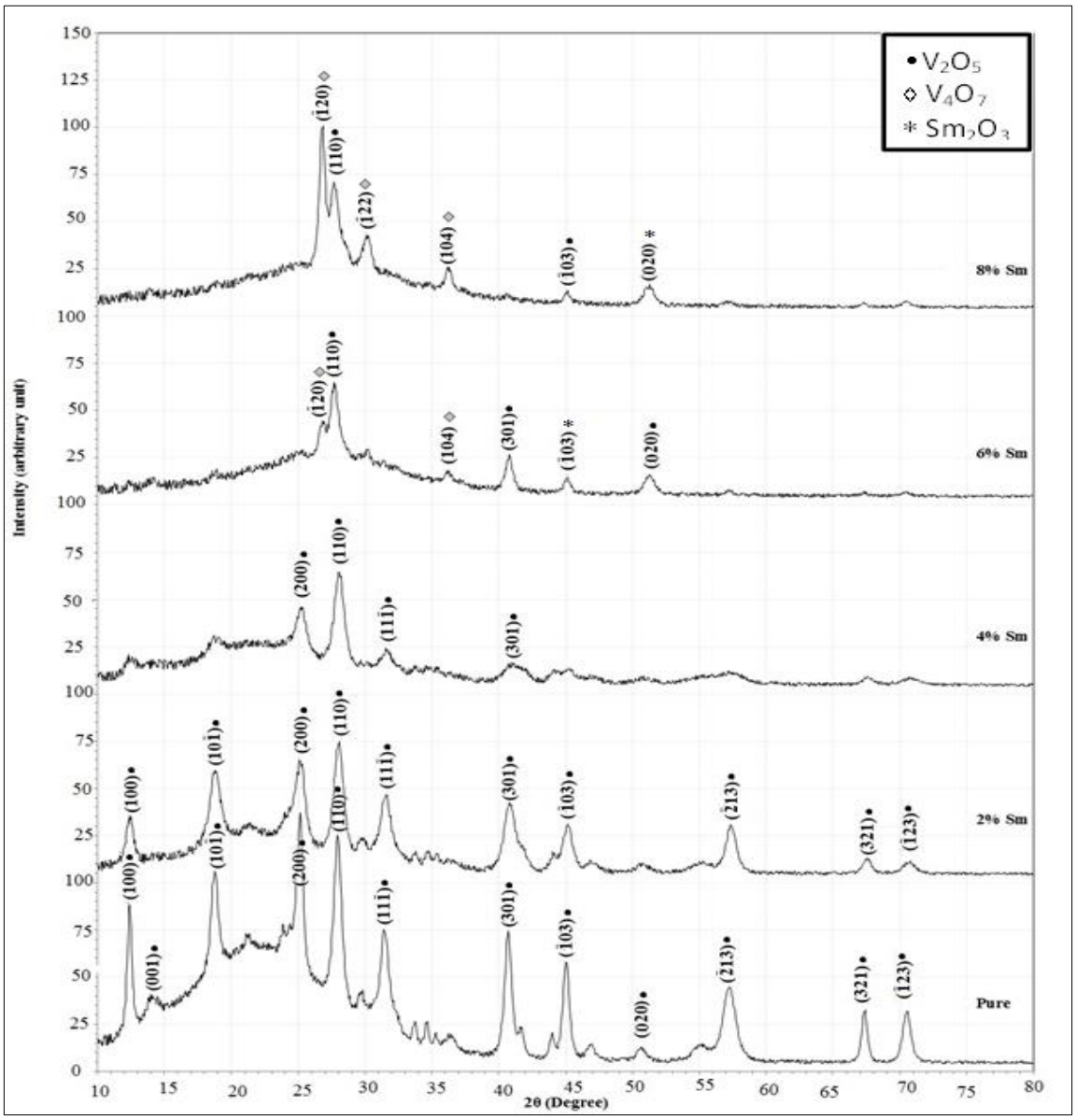

Figure 1. XRD for V_2O_5: Sm_2O_3 at annealing temperature of 400 °C.

The x-ray information of thin films distinguishable with that for known V_2O_5 monoclinic structure and Sm_2O_3 cubic structure as stated by universal centers for Diffraction information ICDD (96-210-2584). this expanding of different doping concentrations of Sm_2O_3 lead to decrease the V_2O_5 peak intensity, as well as, the Sm_2O_3 peaks would be showing up during high concentrations. Table (1) Shows the crystalline size and hkl of Sm_2O_3 doped V_2O_5. At the doping to 6%, two peaks with a low intensity at about (2θ) equivalent to: 26.795°and 36.250° for the planes ($1\bar{2}0$) and (104) with property of V_4O_7, as indicated by the ICDD(NO.96-100-8026), which denote that influence of doping has prompted the development of new phase structure in V_4O_7 films and the atoms of doped material have s effectively come in the Vanadium Oxide host lattice. (Zhao et al., 2011).

Table 1. Values of X-ray diffraction peaks for V_2O_5 films with distinctive doping concentrations of Sm_2O_3 at 400 °C.

Sm_2O_3%	2θ {Deg.}	FWHM {Deg.}	$d_{h.k.l}$ Exp.{Å}	C-S {nm}	h.k.l	$D_{h.k.l}$ Std.(Å)	phase	Caed no.
Pure	12.389	0.416	7.138	19.2	(100)	7.114	V_2O_5	96-210-2584
	14.059	1.111	6.294	7.2	(001)	6.284	V_2O_5	96-210-2584
	18.747	0.626	4.729	12.9	(10-1)	4.712	V_2O_5	96-210-2584
	25.158	0.485	3.536	16.8	(200)	3.557	V_2O_5	96-210-2584
	27.962	0.690	3.188	11.9	(110)	3.192	V_2O_5	96-210-2584
	31.469	0.691	2.840	11.9	(11-1)	2.846	V_2O_5	96-210-2584
	40.710	0.625	2.214	13.6	(301)	2.217	V_2O_5	96-210-2584
	45.039	0.553	2.011	15.5	(-103)	2.008	V_2O_5	96-210-2584
	50.651	0.761	1.800	11.5	(020)	1.611	V_2O_5	96-210-2584
	57.240	1.110	1.608	8.2	(-213)	1.611	V_2O_5	96-210-2584
	67.354	0.485	1.389	19.7	(321)	1.391	V_2O_5	96-210-2584
	70.518	0.693	1.334	14.0	(-123)	1.335	V_2O_5	96-210-2584
2%	12.420	0.631	7.120	12.7	(100)	7.114	V_2O_5	96-210-2584
	18.794	0.949	4.717	8.5	(10-1)	4.712	V_2O_5	96-210-2584
	25.221	0.735	3.528	11.1	(200)	3.557	V_2O_5	96-210-2584
	28.033	0.857	3.180	9.6	(110)	3.192	V_2O_5	96-210-2584
	31.548	0.822	2.833	10.0	(11-1)	2.846	V_2O_5	96-210-2584
	40.813	0.947	2.209	8.9	(301)	2.217	V_2O_5	96-210-2584
	45.152	0.839	2.006	10.3	(-103)	2.008	V_2O_5	96-210-2584
	57.383	0.872	1.604	10.4	(-213)	1.611	V_2O_5	96-210-2584
	67.523	0.735	1.386	13.0	(321)	1.391	V_2O_5	96-210-2584
	70.695	1.051	1.331	9.3	(-123)	1.335	V_2O_5	96-210-2584
4%	25.256	0.843	3.523	9.7	(200)	3.557	V_2O_5	96-210-2584
	28.072	0.896	3.176	9.1	(110)	3.192	V_2O_5	96-210-2584
	31.592	0.860	2.829	9.6	(11-1)	2.846	V_2O_5	96-210-2584
	40.870	1.281	2.206	6.6	(301)	2.217	V_2O_5	96-210-2584
6%	26.795	0.598	3.324	13.7	(-120)	3.327	V_4O_7	96-100-8026
	27.680	0.643	3.220	12.7	(110)	3.192	V_2O_5	96-210-2584
	36.250	0.631	2.476	13.2	(104)	2.478	V_4O_7	96-100-8026
	40.699	0.518	2.215	16.3	(301)	2.217	V_2O_5	96-210-2584
	45.025	0.459	2.011	18.7	(-103)	2.008	V_2O_5	96-210-2584
	51.246	0.920	1.781	9.6	(020)	1.611	V_2O_5	96-210-2584
8%	26.795	0.500	3.324	16.3	(-120)	3.327	V_4O_7	96-100-8026
	27.680	0.675	3.220	12.1	(110)	3.192	V_2O_5	96-210-2584
	30.167	0.683	2.960	12.0	(1-22)	2.970	V_4O_7	96-100-8026
	36.250	0.631	2.476	13.2	(104)	2.478	V_4O_7	96-100-8026
	45.180	0.560	2.005	15.4	(-103)	2.008	V_2O_5	96-210-2584
	51.246	0.920	1.781	9.6	(020)	1.611	V_2O_5	96-210-2584

Figure. (2) indicates FESEM images to V_2O_5 thin films at different Sm_2O_3 concentrations 0%,2%,4%,6%, and 8% wt.%. Every last one of images seemed in fig. (2) appears homogeneous group distribution with columnar structure while for pure V_2O_5 image the structure revealed some holes; where the average grain size values decrease slightly with increasing doping. The significant change in the average value of cluster surface with increasing Sm_2O_3 proportion. The least cluster surface showed up maximum doping proportion 8% while maximum cluster surface appeared to least doping proportion 2%. The no. of clusters per image appears reversible conduct comparing to the average of cluster surface with increasing of doping. These behaviors indicate increasing the surface of cluster boundaries where the grains didn't bring enough energy to enucleation to decrease cluster

area surface. Expanding Sm_2O_3 proportion prompts increment number of Sm_2O_3 molecules on the substrate surface which act as traps for add atoms causing to decrease grain size by extent toward expanding amount about nucleation centers prompts making another phase from vanadium oxide likewise. It is clear from the figure (2)that the particle size decreases with the increase of samarium oxide concentration.

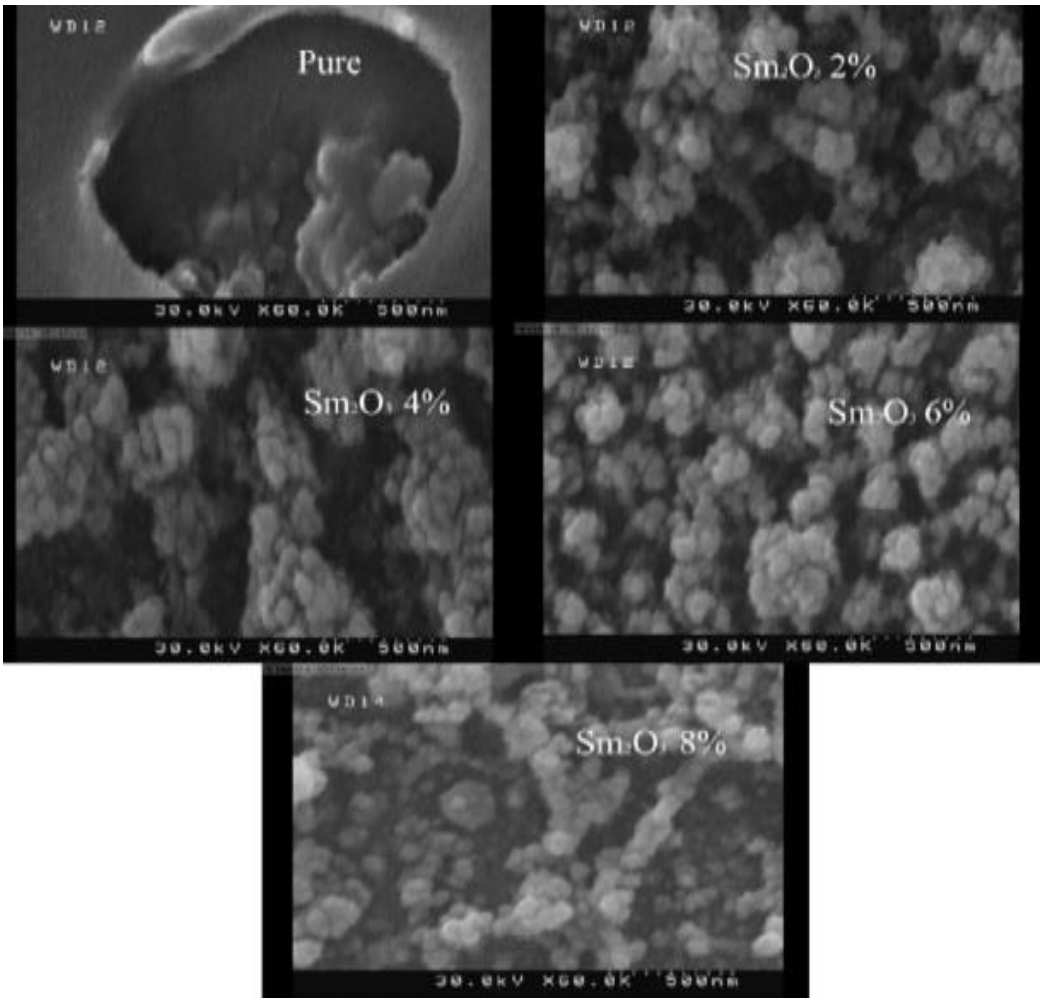

Figure 2. FESEM for V_2O_5:Sm_2O_3 with different Sm_2O_3 ratios

The optical band gap (E_g^{opt}), which might assistance evaluate the electronic what's more thermoelectric characteristic about materials (Isam et al., 2018). The optical energy gap (E_g^{opt}) have been evaluated utilizing Tauc equation by the extrapolation of the parcel at $(\alpha h\upsilon)^2 = 0$. The energy gap expanding with expand of doping concentration starting with 2.610 eV to 2.7 eV as shown in Figures (3). It observed that (E_g opt) will be expanding marginally, furthermore shifting towards the ultra-violate- range, this may be due to the impact from impurity or disorder. Also, whatever available defects, semiconductors prompt to local electric fields that influence the band tails close to the band edge. Likewise, the measure impact to nanostructure produce this shift. The results of energy gap show that the prepared thin films have localized states which result from the density of defects at the grain boundaries furthermore donor levels, along these lines we might that those optical energy gap could a chance to be controlled through impurities proportions and the particle size of nanostructure, in addition the variation of the crystallite size expanding of energy gap place by the effect of quantum confinement.

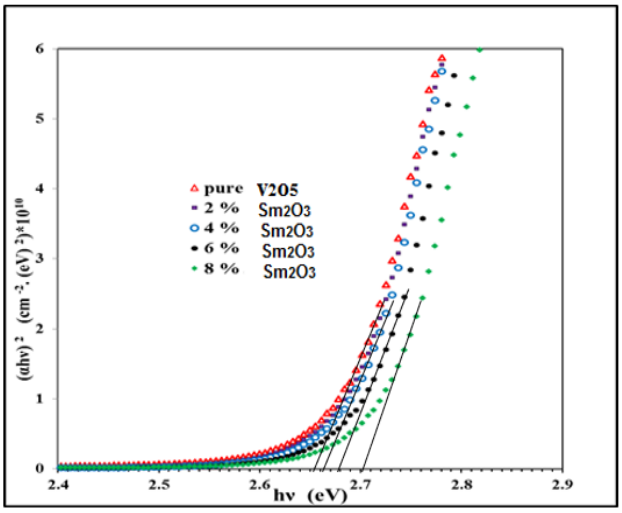

Figure 3. $(\alpha h\upsilon)^2$ against photon energy ($h\upsilon$) for V_2O_5 films at (2, 4, 6, and 8) wt. % Sm_2O_3 proportion

Figure (4,5,6and 7) indicates the sensing conduct about pure V_2O_5 and doping with Sm_2O_3 /Si for NO_2 gas, it is clear from this figure that the resistance increases with gas on till reach the maximum value and the behavior will be opposite for gas shutting. From figures it is found that greatest sensitivity about 99%, and the response time equivalent to 10s, while, recovery time 18s for 4% Sm_2O_3 sample at 50 °C In general, the mechanism of V2O5 is identified with the ionosorption for gas species through the surface, prompting to charge exchange of the gas and surface. Particles Moreover progressions in the electrical conductance (Filipovic et al., 2013). Figures show that the increases in the resistance value when their films presentation to NO_2gas, {Gas ON}, After that the resistance again sloping at the shutdown of the gas {Gas OFF}. This behavior can be attributed to the subsequent (NO_2) gas that undergoes an ionic reaction with surface adsorption oxygen, these electrons on oxygen can be concentrated starting from the semiconductor materials, the electrical conductivity of V_2O_5 materials will decrease causing the increasing in resistance (Filipovic et al., 2013). The variable resistance value indicated by this metal oxide sensor in the air, oxygen is adsorbed on the surface, besides the formation of dissociates (O-), the place where the electron is on the oxygen can be concentrated starting from these semiconductors. This electron resorts to increasing the resistance of n-type semiconductors, where electrons are the main carriers. For gas (NO_2), nitrogen reacts to adsorbed (O-) to form NO_2, and an electron can be reintroduced under these semiconductors, resorting to decreasing resistance. The adversary acts on the middle of the oxygen, removing electrons, and the combustible gas restores these electrons. Thus, the consistent quality of resistance of the metal oxide depends on the fixation of the flammable gas. However, it can be seen from the table below that the addition of samarium to vanadium oxide at any concentration does not have a significant effect.

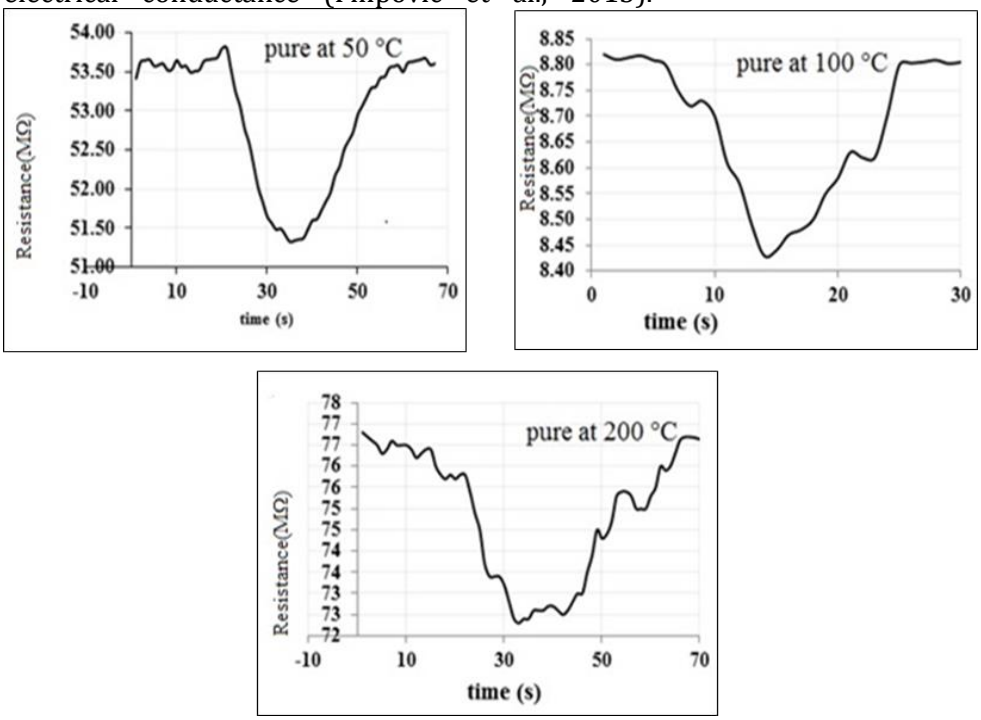

Figure 4. Variety for resistance as a function to the time pure V2O5 films at 50,100 and 200 °C

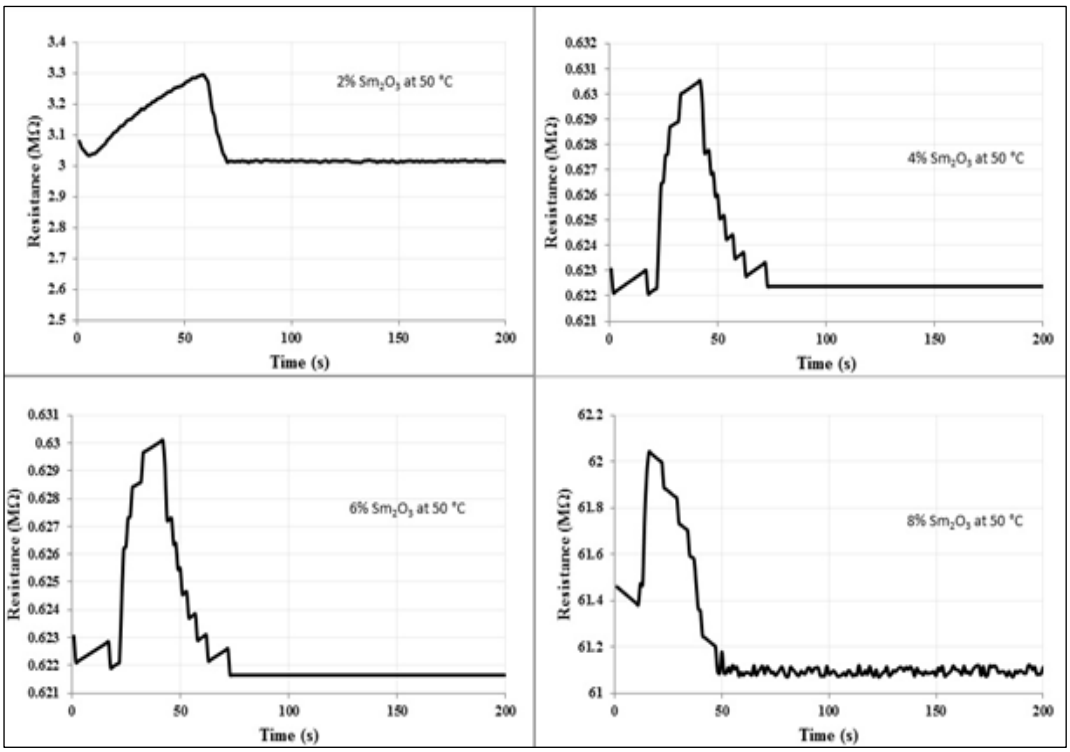

Figure 5. Variety for resistance as a function of time V_2O_5 films with (2, 4, 6, and 8) wt. %. Sm_2O_3 ratio at 50 °C

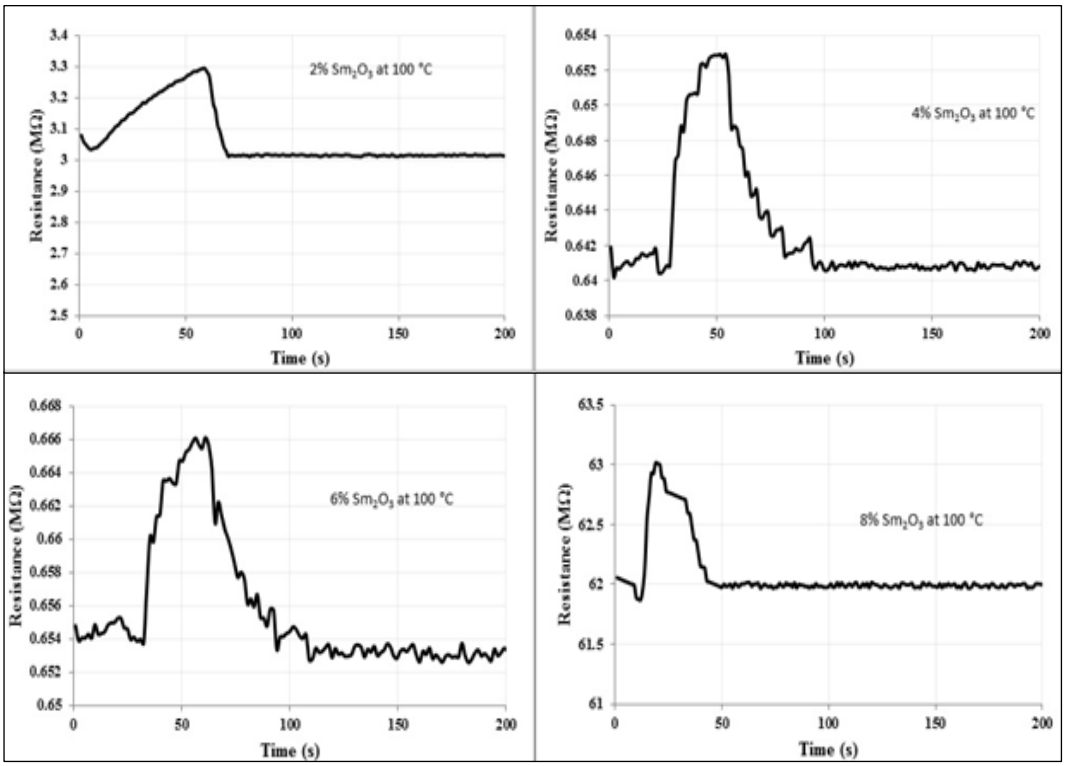

Figure 6. Variety for resistance as a function of time V_2O_5 films with (2, 4, 6, and 8) wt. %. Sm_2O_3 ratio at 100 °C.

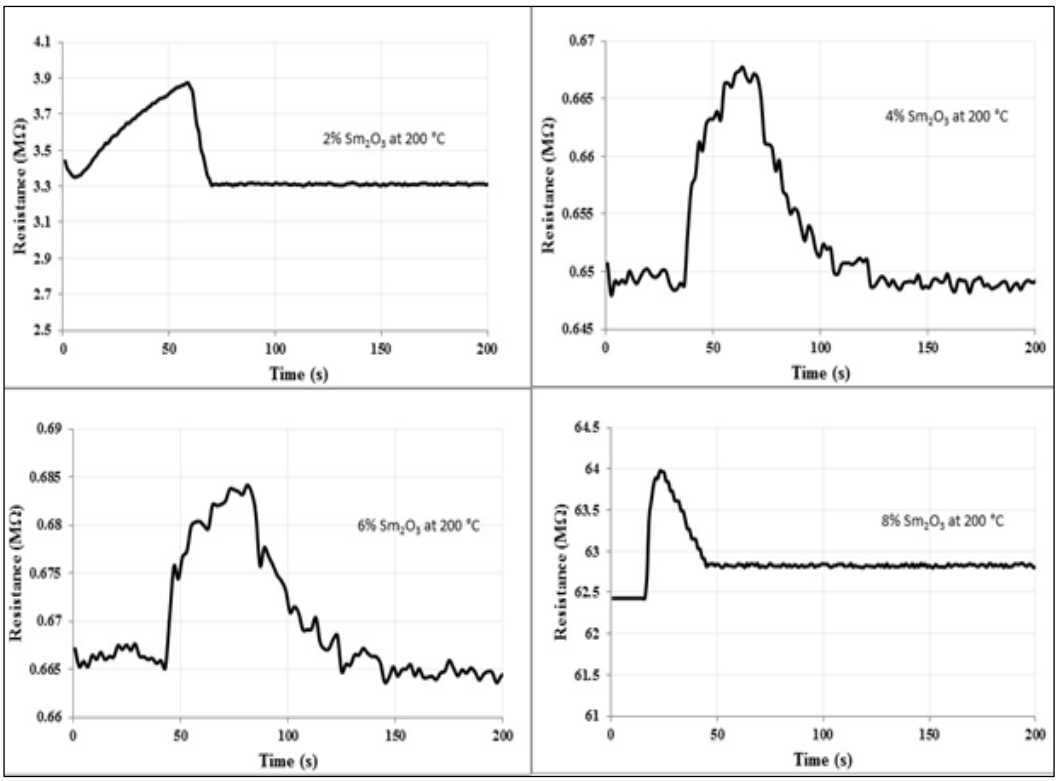

Figure 7. Variety for resistance as a function to the time V_2O_5 films with (2, 4, 6, and 8) wt. %. Sm_2O_3 ratio at 200 Cº

Table 2. Indicates the sensitivity, response and recovery time of V_2O_5 films with (2, 4, 6, and 8) wt. %. Sm_2O_3 ratio

	Sensitivity%			Response			Recovery		
	50Cº	100 Cº	200 Cº	50 Cº	100 Cº	200 Cº	50 Cº	100 Cº	200 Cº
PURE	96	96	95	18	8	21	27	7	23
2%	96	93	88	50	53	53	10	12	13
4%	99	98	97	10	14	25	18	19	43
6%	99	98	97	13	17	20	16	27	30
8%	99	98	98	8	10	8	30	21	21

Conclusions

V2O5:Sm2O3 thin films were prepared, using Pulsed Laser deposition method successfully. X-ray diffraction declared V_2O_5 monoclinic structure, as well as another phase V_4O_7 appeared at high doping ratio of Sm_2O_3, the appearance attributed to the abundance of oxygen supplied from the heat treatment as well as from the Sm_2O_3. FESEM images indicate homogeneous bunch distribution for columnar structure and the average grain size values decrease slightly for increment doping. The blue shift of E_g is attributed to the quantum confinement effect. The sensing behavior NO_2 gas of V_2O_5 doped with Sm_2O_3 /Si for NO_2 gas increases with doping ratio till reach steady value 99% give indication that the surface of gas sensors cells reach saturation, the response time equivalent to 10s at doping ratio 8% at working temperature 50 °C.

References

Benmoussa M, Outzourhit A, Bennouna A, Ameziane EL. Electrochromism in sputtered V_2O_5 thin films: structural and optical studies. *Thin Solid Films* 2002; 405(1-2): 11-16.

Zou CW, Gao W. Fabrication, optoelectronic and photocatalytic properties of some composite oxide nanostructures. *Transactions on electrical and electronic materials* 2010; 11(1): 1-10.

Londero E, Schröder E. Role of van der Waals bonding in the layered oxide V_2O_5: First-principles density-functional calculations. *Physical Review B* 2010; 82(5): 054116.

Ali IM, Rzaij JM, Abbas QA, Ibrahim IM, Alatta HJ. Structural, optical and sensing behavior of neodymium-doped vanadium pentoxide thin films. *Iranian Journal of Science and Technology, Transactions A: Science*, 2018; 42(4): 2375-2386.

Bhushan B. *Hand Book of Nanotechnology*. Springer 2007.

Bochenkov VE, Sergeev GB. Sensitivity, selectivity, and stability of gas-sensitive metal-oxide nanostructures. *Metal oxide nanostructures and their applications* 2010; 3: 31-52.

Gibbs ZM, LaLonde A, Snyder GJ. Optical band gap and the Burstein–Moss effect in iodine doped PbTe using diffuse

reflectance infrared Fourier transform spectroscopy. *New Journal of Physics* 2013; 15(7): 075020.

Zhao J, Ni J, Zhao X, Xiong Y. Preparation and characterization of transparent conductive zinc doped tin oxide thin films prepared by radio-frequency magnetron sputtering. *Journal of Wuhan University of Technology-Mater Science Education* 2011; 26(3): 388-392.

Isam MI, Abubaker SM, Asmiet R. Energy Band Diagram of NiO: Lu2 O3/n-Si heterojunction. *Iraqi Journal of Science* 2018; 59(1B): 287-293.

Filipovic L, Selberherr S, Mutinati GC, Brunet E, Steinhauer S, Köck A, Grogger W. A method for simulating spray pyrolysis deposition in the level set framework. *Engineering Letters* 2013; 21(4): 224-240.

Marchionni M, Caramel S, Stagnaro S. Inherited real risk of schizophrenia: Pathogenesis, bedside diagnosis and primary prevention. *NeuroQuantology* 2019; 17(5): 10-16.

Saniotis A. Becoming animals: Neurobiology of shamanic shapeshifting. *NeuroQuantology* 2019; 17(5): 81-86.